WIND TUNNEL AEROELASTIC ANALYSIS OF A LOW-STIFFNESS WING AT HIGH ANGLES OF ATTACK AND LOW REYNOLDS NUMBERS

Mindaugas Dagilis*, Martynas Lendraitis and Sigitas Kilikevičius

*only the affiliation and address of the corresponding author

Kaunas university of technology,
Studentu g. 56-232, LT-51424, Kaunas
Lithuania

ABSTRACT

Computationally efficient aeroelasticity modeling is of high interest for early phases of aircraft design, and for control law design (such as active flutter suppression or gust load alleviation). These processes are highly iterative, and high fidelity CFD based aeroelasticity models are usually not viable. A lot of research is being published describing different methods of computationally efficient aeroelastic modeling [1-6]. Experimental aeroelasticity research is very important for providing data used for developing and validating such models. One recent successful example would be the Pazy wing study [7].

However, most currently published low fidelity aeroelasticity models use linear aerodynamics. While this is accurate for most real flight conditions, it introduces significant errors at low Reynolds numbers and high angles of attack. Aeroelasticity models that would take aerodynamic non-linearities into account could potentially be useful for designing aeroelastic control laws at the edges of the aircraft's flight envelope. To develop such models, experimental aeroelasticity data from highly aerodynamically non-linear test cases is required. This paper describes such a wind tunnel study, analyzing a low-stiffness wing at high angles of attack and low Reynolds numbers.

The structure of the wind tunnel model is based on the Pazy wing [7]. The picture of the analyzed wing can be seen in Fig. 1. The wing has a rectangular planform, a span of 320 mm, and a chord of 50 mm. The NACA 0018 airfoil is used along the full span. The main structural element is a stainless steel spar, which is 40 mm wide, 0.5 mm thick, and extends the full span of the wing. The spar also extends past the root of the wing and is used to fix it in the wind tunnel. 3D printed wing ribs are mounted on this spar with 20 mm spacing. The trailing and leading edges of each rib is extended to connect to the next rib. The wing is covered with a heat-shrink film to form the outer aerodynamic shape. At the wingtip, a 100 mm long M4 threaded rod is mounted that can be used to attach additional weights. Three accelerometers are attached near the wingtip. Two are mounted close to the leading and the trailing edges and are aligned to measure out-of-plane accelerations. One is mounted at the mid-chord and is aligned to measure in-plane accelerations. The mass of the wing without any wingtip masses attached is 71.5 g. The threaded wingtip rod adds an additional 7.0 g, and the two weights centered 43 mm from the mid-chord add 5.3 g each, for a total mass of 89.1 g.

Fig. 1 Analyzed wind tunnel model

Impact response testing of the wing was performed to determine the structural frequencies without any air flow. It was found that the five lowest structural frequencies included three out-of-plane bending modes at 2.85 Hz, 23.6 Hz and 70.7 Hz, one torsional mode at 27.6 Hz and one in-plane bending mode at 50.5 Hz.

The tests are conducted at the Lithuanian Energy Institute wind tunnel. The tunnel is of the closed-return type and has an open test section. The diameter of the tunnel as it enters the test section is 400 mm. The maximum achievable air speed is 40 m/s. An ultrasound anemometer is installed in the wind tunnel for accurate speed measurement.

The tests are conducted at angles of attack from 0° to 15°, with an interval of 2.5°. At each angle of attack, the initial air speed is set to 11.8 m/s (minimum possible without additional mesh in the wind tunnel), which is first increased to 13.0 m/s, and then further increased with an interval of 2.0 m/s, reducing the interval if strong changes in the aeroelastic behavior are observed. At each air speed, the output of the accelerometers is measured 5 times for 5 s, at a sampling rate of 10 kHz. If flutter is not observed during a given test case, the wing is impacted to measure the frequency response.

An analysis of the displacement of the wingtip was performed based on video of the wind tunnel tests. It was found that the maximum wingtip displacement for a fixed airspeed was achieved at 10°, confirming that the wing was operating in the aerodynamically non-linear region at the high angles of attack.

At all tested angles of attack, second out-of-plane bending mode flutter was observed. The dependence of flutter speed (in the second bending mode) on the angle of attack is shown in Fig. 2. The highest flutter speed was 26.6 m/s, observed at 0° angle of attack, it decreased sharply to 18.9 m/s at 2.5°, and continued gradually decreasing until 12.5°, then slightly increased again at 15°. At 12.5°, first out-of-plane bending mode flutter was also observed, already present at the initial speed of 11.8 m/s. As the air speed increased, flutter switched from the first to the second out-of-plane mode.

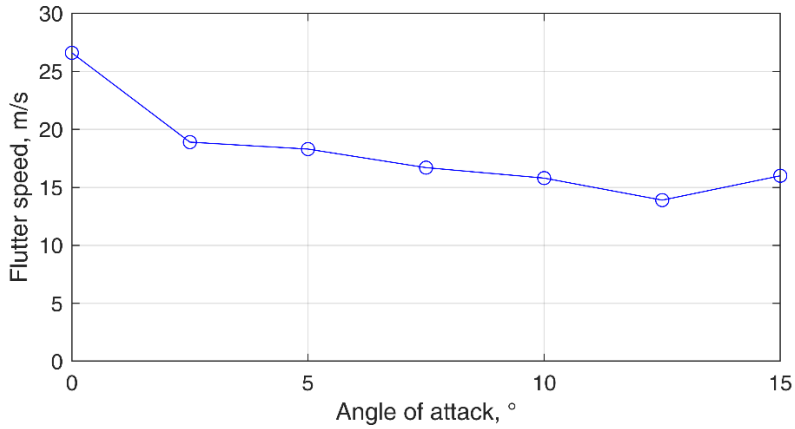

Fig. 2 Second out-of-plane bending mode flutter speed change with angle of attack

When performing the frequency analysis of the wing in an air flow, it was found that as the air speed increased, the second out-of-plane bending and first torsion frequencies approached each other, and as the wing entered flutter, they merged into a single frequency. At the same time, the frequency of the first in-plane mode shifted to exactly twice the base flutter frequency. In general, a large shift in the structural frequencies of the wing was not observed either as the air speed increased, or when comparing different angles of attack at the same air speed.

In conclusion, the performed wind tunnel tests appear to capture the aerodynamically non-linear

aeroelastic behavior of a wing in a high angle of attack, low Reynolds flow. The results of this experimental study can be used to develop and validate aeroelasticity models based on non-linear aerodynamics. The authors of this paper are currently developing such a model. Such models can in turn be used to designing control laws which would work effectively at the edges of an aircraft's flight envelope.

ACKNOWLEDGEMENT

This research received funding from the Research Council of Lithuania (LMTLT), agreement No. S-MIP-24-44.

REFERENCES

1. Alvaro Cea and Rafael Palacios. JAX-based aeroelastic simulation engine for differentiable aircraft dynamics. Computer Physics Communications, 311:109547, June 2025.
2. M.K. Hickner, U. Fasel, A.G. Nair, B.W. Brunton, and S.L. Brunton. Data-Driven Unsteady Aeroelastic Modeling for Control. AIAA Journal, 61(2):780-792, 2023.
3. J.A. Grauer and M.J. Boucher. Real-time estimation of bare-airframe frequency responses from closed-loop data and multisine inputs. Journal of Guidance, Control, and Dynamics, 43(2):288-298, 2020.
4. Zexuan Yang, Chao Yang, Daxin Wen, Wenbo Zhou, and Zhigang Wu. A Time-Domain Calculation Method for Gust Aerodynamics in Flight Simulation. Aerospace, 11(7):583, July 2024.
5. Alvaro Cea, Rafael Palacios, and Lucian Iorga. Near-Real-Time Nonlinear Analysis of Free-Flying Flexible Aircraft on Modern Hardware Architectures. AIAA Journal, October 2025.
6. Mindaugas Dagilis, Martynas Lendraitis and Sigitas Kilikevičius. Feasibility of Real-time Aeroelasticity Modeling Using the Unsteady Vortex Lattice Method. AIAA Aviation Forum and ASCEND 2025. American Institute of Aeronautics and Astronautics, July 2025.
7. Markus Ritter et al. Collaborative Pazy Wing Analyses for the Third Aeroelastic Prediction Workshop. AIAA SCITECH 2024 Forum. American Institute of Aeronautics and Astronautics, January 2024.